

# Human Activity Recognition with Convolutional Neural Networks<sup>\*</sup>

Antonio Bevilacqua<sup>1</sup>, Kyle MacDonald<sup>2</sup>, Aamina Rangarej<sup>2</sup>, Venessa Widjaya<sup>2</sup>, Brian Caulfield<sup>1</sup>, and Tahar Kechadi<sup>1</sup>

<sup>1</sup> Insight Centre for Data Analytics, UCD, Dublin, Ireland

<sup>2</sup> School of Public Health, Physiotherapy and Sports Science, UCD, Dublin, Ireland

**Abstract.** The problem of automatic identification of physical activities performed by human subjects is referred to as Human Activity Recognition (HAR). There exist several techniques to measure motion characteristics during these physical activities, such as Inertial Measurement Units (IMUs). IMUs have a cornerstone position in this context, and are characterized by usage flexibility, low cost, and reduced privacy impact. With the use of inertial sensors, it is possible to sample some measures such as acceleration and angular velocity of a body, and use them to learn models that are capable of correctly classifying activities to their corresponding classes. In this paper, we propose to use Convolutional Neural Networks (CNNs) to classify human activities. Our models use raw data obtained from a set of inertial sensors. We explore several combinations of activities and sensors, showing how motion signals can be adapted to be fed into CNNs by using different network architectures. We also compare the performance of different groups of sensors, investigating the classification potential of single, double and triple sensor systems. The experimental results obtained on a dataset of 16 lower-limb activities, collected from a group of participants with the use of five different sensors, are very promising.

**Keywords:** human activity recognition · cnn · deep learning · classification · imu

## 1 Introduction

Human activity recognition (HAR) is a well-known research topic, that involves the correct identification of different activities, sampled in a number of ways. In particular, sensor-based HAR makes use of inertial sensors, such as accelerometers and gyroscopes, to sample acceleration and angular velocity of a body. Sensor-based techniques are generally considered superior when compared with other methods, such as vision-based, which use cameras and microphones to record the movements of a body: they are not intrusive for the users, as they do not involve video recording in private and domestic context, less sensitive to

---

<sup>\*</sup> This study was approved by the UCD Office of Research Ethics, with authorization reference LS-17-107.

environmental noise, cheap and efficient in terms of power consumption [8, 13]. Moreover, the wide diffusion of embedded sensors in smartphones makes these devices ubiquitous.

One of the main challenges in sensor-based HAR is the information representation. Traditional classification methods are based on features that are engineered and extracted from the kinetic signals. However, these features are mainly picked on a heuristic base, in accordance with the task at hand. Often, the feature extraction process requires a deep knowledge of the application domain, or human experience, and still results in shallow features only [5]. Moreover, typical HAR methods do not scale for complex motion patterns, and in most cases do not perform well on dynamic data, that is, data picked from continuous streams.

On this regard, automatic and deep methods are gaining momentum in the field of HAR. With the adoption of data-driven approaches for signal classification, the process of selecting meaningful features from the data is deferred to the learning model. In particular, CNNs have the ability to detect both spatial and temporal dependencies among signals, and can effectively model scale invariant features [15].

In this paper, we apply convolutional neural networks for the HAR problem. The dataset we collected is composed of 16 activities from the Otago exercise program [12]. We train several CNNs with signals coming from different sensors, and we compare the results in order to detect the most informative sensor placement for lower-limb activities. Our findings show that, in most scenarios, the performance of a single sensor is comparable to the performance of multiple sensors, but the usage of multiple sensor configurations yields slightly better results. This suggests that collinearities exist among the signals sampled with sensors on different placements.

The rest of the paper is organized as follows: Section 2 gives a brief overview of the state of the art of deep learning models for activity recognition. Section 3 presents our dataset, the architecture of our neural network, and the methodology adopted in this study. The experimental results are discussed in Section 4. Some concluding remarks and future extensions for this study are provided in Section 5.

## 2 Related works

Extensive literature has been produced about sensor-based activity recognition. Bulling *et al.* [6] give a broad introduction to the problem, highlighting the capabilities and limitations of the classification models based on static and shallow features. Alsheikh *et al.* [2] introduce a first approach to HAR based on deep learning models. They generate a spectrogram image from an inertial signal, in order to feed real images to a convolutional neural network. This approach overcomes the need for reshaping the signals in a suitable format for a CNN, however, the spectrogram generation step simply replaces the process of feature extraction, adding initial overhead to the network training. Zeng *et al.* [15] use

raw acceleration signals as input for a convolutional network, applying 1-D convolution to each signal component. This approach may result in loss of spatial dependencies among different components of the same sensor. They focus on public datasets, obtained mainly from embedded sensors (like smartphones), or worn sensors placed on the arm. A similar technique is suggested by Yang *et al.* [14]. In their work, they use the same public datasets, however, they apply 2-D convolution over a single-channel representation of the kinetic signals. This particular application of CNNs for the activity recognition problem is further elaborated by Ha *et al.* [10], with a multi-channel convolutional network that leverages both acceleration and angular velocity signals to classify daily activities from a public dataset of upper-limb movements. The classification task they perform is personalized, so the signals gathered from each participant are used to train individual learning models.

One of the missing elements in all the previously described contributions about deep learning models is a comparison of the classification performance of individual sensors or group of sensors. Our aim in this paper is to implement a deep CNN that can properly address the task of activity recognition, and then compare the results obtained with the adoption of different sensor combinations. We also focus on a set of exercise activities that are part of the Otago exercise program. To the best of our knowledge, this group of activities has never been explored before in the context of activity recognition.

### 3 Data and methodology

The purpose of this paper is to assess the classification performance of different groups of IMU sensors for different activities. We group the target activities into four categories, and, for each category, we aim at identifying the best placement for the inertial units, as well as the most efficient combination of sensors, with respect to the activity classification task.

#### 3.1 Sensors and data acquisition

Five sensors were used for the data collection phase. Each sensor is held in place by a neoprene sleeve. For this study, we set the placement points as follows:

- two sensors placed on the distal third of each shank (left and right), superior to the lateral malleolus;
- two sensors centered on both left and right feet, in line with the head of the fifth metatarsal;
- one sensor placed on the lumbar region, at the fourth lumbar vertebrae.

We explore three main sensor configurations: with a **single device** setup, we classify the activity signal coming from each individual sensor. In the **double device** setup, four combinations of two sensors are tested: shin sensors (right and left), foot sensors (right and left), right sensors and left sensors (foot and

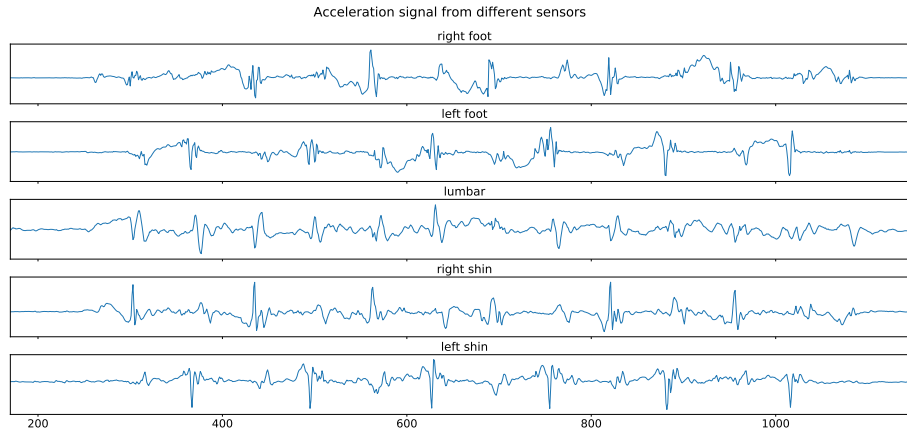


Fig. 1: This acceleration  $x$  components correspond to roughly 10 seconds of activity, acquired with the five sensors used in this study. Signals sampled by different sensors may show very discordant patterns and characteristics.

shin). When testing the **triple device** setups, the lumbar sensor is included in each one of the double sensor configurations.

The chosen device for this study is Shimmer3 [7]. The Shimmer3 IMU contains a wide set of kinetic sensors, but we are interested in sampling acceleration and angular velocity only. Both these quantities are captured by triaxial sensors, so each Shimmer3 device returns a set of six signals (three acceleration components, over the axes  $x$ ,  $y$  and  $z$ , and three angular velocity components, over the same axes). The sampling rate is set to 102.4 Hz for all sensors. The accelerometer is configured to have a range of  $\pm 2g$ , while the gyroscope range is set to 500 dps. We adopted this particular configuration in order to avoid aliasing when sampling the target activities, as gait-related human motion usually locates in the frequency range of 0.6-5.0 Hz [9].

### 3.2 Target activities and population

The physical activities targeted in this paper are part of the Otago Exercise Programme (OEP), a programme of activities designed to reduce the risk of falling among the elderly [12]. In particular, we grouped 16 different activities into four categories: **walk**, **walking balance**, **standing balance**, and **strength**. None of the Otago warm up activities is included in this study.

**Walk** : it is composed of backwards walking (bawk), sideways walking (sdwk), walking and turning around (wktrn). These three activities have all wide and diverse range of movements, especially for the foot sensors.

**Walking Balance** : it is composed of heel to toe walking backwards (het-owkbbk), heel walking (hewk), tandem walking (tdwk), toe walking (towk). These activities are based on similar ranges of movements.

**Standing Balance** : it is composed of single leg stance (sls), and tandem stance (tdst). The signals sampled from these two activities are mainly flat, as they require the subject to move only once in order to change the standing leg from left to right.

**Strength** : it is composed of knee extension (knex), knee flexion (knfx), hip abduction (hpabd), calf raise (cars), toe raise (tors), knee bend (knbn), and sit to stand (std). As some of these activities are performed by using each individual leg separately, all the sensor configurations involving both right and left sides are not applicable for this group.

A standard operating procedure defines the execution setup for all the target activities, in terms of holding and pausing times, overall duration, starting and ending body configurations. The same operating procedure is applied to all the subjects involved in the study.

The group of 19 participants consists of 7 males and 12 females. Participants have a mean age of  $22.94 \pm 2.39$ , a mean height of  $164.34 \pm 7.07$  cm, and a mean weight of  $66.78 \pm 11.92$  kg.

### 3.3 Dataset

Once the signal is acquired from the activity, it is segmented into small overlapping windows of 204 points, corresponding to roughly 2 seconds of movements, with a stride of 5 points. A reduced size of the windows is generally associated with a better classification performance [3], and in the context of CNNs, it facilitates the training process as the network input has a contained shape. Therefore, each window comes in the form of a matrix of values, of shape  $6N \times 204$ , where  $N$  is the number of sensors used to sample the window. The dense overlapping among windows guarantees high numerosity of training and testing samples. As the activities have different execution times, and different subjects may execute the same activity at different paces, the resulting dataset is not balanced. The distributions of the example windows over the activity classes for the five target groups are listed in table 1.

For assessing the performance of our classification system, we use a classic 5-fold cross-validation approach. We partition the available datasets based on the subjects rather than on the windows. This prevents overfitting over the subjects, and helps to achieve better generalisation results. In this regard, 4 participants out of 19 are always kept isolated for testing purposes, so each fold is generated with an 80/20 split.

### 3.4 Input adaptation and network architecture

The shape of the input examples that is fed to the network depends on the sensor configuration, as each sensor samples 6 signal components that are then arranged into a  $6 \times 204$  single-channel, image-like matrix, as described in Section 3.3. Therefore, the input of the network has shape  $6 \times 204 \times N$ , where  $N$  is the number of channels and is equal to the number of sensors used for the sampling. This

Table 1: Label distributions for the activity groups

activity	windows	percentage	activity group	total
bawk	19204	39.88	walk	48143
sdwk	22077	45.85		
wktrn	6925	14.38		
hetowk	4130	9.44	walk balance	43754
hewk	17796	40.67		
tdwk	4578	10.46		
towk	17250	39.42		
sls	20006	65.05	stand balance	30759
tdst	10753	34.95		
knex	7500	12.14	strength	76854
knfx	6398	10.42		
hpabd	5954	9.62		
cars	6188	10.11		
tors	5815	9.41		
knbn	26452	34.42		
sts	8533	13.86		

input adaptation is known as model-driven [13], and it is effective in detecting both spatial and temporal features among the signal components [10]. Figure 2 shows how the signal components are stacked together and form the input image for the network.

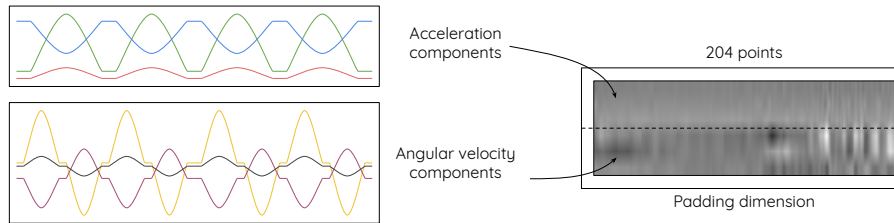


Fig. 2: The signal components are stacked on top of each other to form a bidimensional matrix of values. Additional sensors would generate new channels of the same shape.

The full structure of our convolutional model is shown in Figure 3. After the input layer, three convolutional layers interleave with three max pooling layers. The depthwise convolution operation generates multiple feature maps for every input channel, with kernels of size  $3 \times 5$ ,  $2 \times 4$  and  $2 \times 2$  in the first, second and third convolutional layer respectively. The input of every convolutional layer is properly padded so that no loss of resolution is determined from the convolution

operation. Batch normalization is applied after each convolutional layer. The three max pooling layers use kernels of size  $3 \times 3$ ,  $2 \times 2$  and  $3 \times 2$  respectively. A fully connected network follows, composed by three dense layers of 500, 250 and 125 units. The dense layers are regularized with dropout during the training phase, with a 0.5 probability of keeping each neuron. The ReLU function is used as activation function within the whole network, while the loss is calculated with the cross entropy function. The Adam optimizer is used as stochastic optimization method [11]. The output layer is composed of  $m$  units, where  $m$  corresponds to the number of activities in each group. The softmax function will return the most likely class of the input windows in the multi-class classification task.

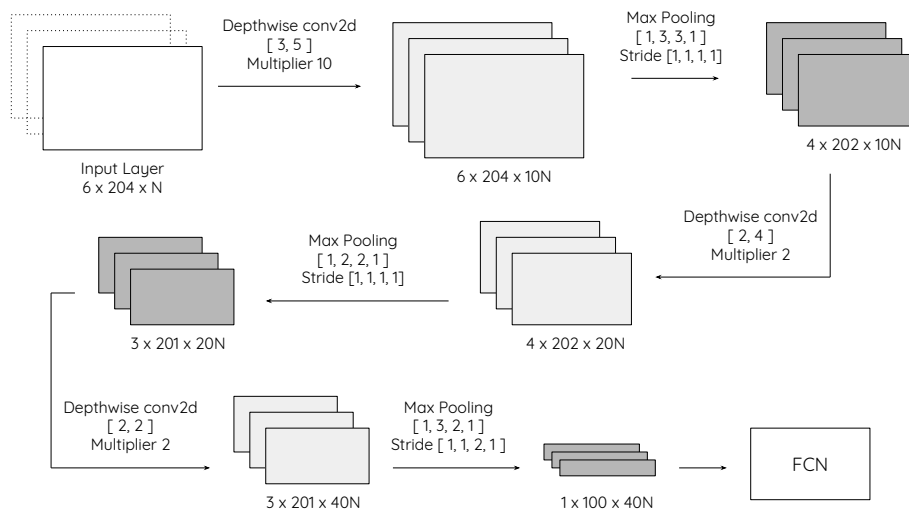


Fig. 3: Our CNN architecture, where  $N$  represents the number of sensors used during the activity sampling. Regardless the value of  $N$ , the network structure does not change, as depthwise convolution applies different filters to each one of the input channels.

We select a set of hyperparameters that are kept constant for all the activity groups and sensor configurations, based on literature best practices [4] and empirical observations. We use a batch size of 1024, as we find this value to speed up the learning process when compared with smaller sizes, without being computationally too complex to manage. The number of training epochs varies from 150 to up to 300, according to the behavior of individual configurations. The initial learning rate is fixed to 0.005. The network is implemented with the TensorFlow framework [1], version 1.7. Our objective is not to build the most performant network for the task, but it is rather to compare the classification potential of

different sensors. The rationale behind our architectural choices relies therefore on a rather standard network configuration, based on small kernels, standard regularization methods, and a compact set of hyperparameters. In our experience, three convolutional layers will lead to overfitting when no regularization method is applied. However, introducing dropout stabilizes the learning, and the network performance does not benefit from the inclusion of further convolutional or dense layers.

## 4 Experimental results

In order to evaluate our classifier, we collect individual precision and recall scores for every combination of sensors and activities, and we then compute the F-scores. A synoptic overview of the results is presented in Figure 4.

In the results shown in Figure 4, the sensor combinations lay on the  $x$  axis. Starting from the left, there are right foot (RF), left foot (LF), right shin (RS), left shin (LS), lumbar (LM), and all the other target setups (for instance, the triple setup on the right side is indicated by RSRFLM, that is, right shin, right foot, lumbar). The activities are arranged on the  $y$  axis. Activity and sensor groups are indicated by the black grid of horizontal and vertical lines. Each tile in the picture contains the F-score obtained for the corresponding activity and sensor configuration. The color gradient of the tiles corresponds to the F-scores, and helps identifying high level performance for activity groups or sensor configurations.

The vertical strip of tiles corresponding to the lumbar sensor (LM) clearly shows that this single sensor does not hold any significant discriminating power, nor it adds meaningful information when included in the triple sensor group, shown in the rightmost region of the picture. Overall, a strong pattern on the sensor configurations does not appear to emerge: the units placed on the feet show very similar results to the units placed on the shins, without clear distinction in terms of discriminating power.

The confusion matrices resulting from the evaluation process over the test datasets are shown in Figures 5, 6, 7 and 8, for the walk group, the walking balance group, the standing balance group, and the strength group respectively. The color gradient for each matrix is normalized on the rows.

The walk group scores interesting results for every sensor configuration. Single sensors perform slightly worse than multiple sensor setups, however, there seems to be no difference between two sensors and three sensors. From the confusion matrix in Figure 5, we observe that the two majority classes, *bawk* and *sdwk*, determined a reasonably limited amount of misclassified instances, while the minority class, *wktrn*, only recorded 4% of false negatives.

The same behavior is shown for the walking balance group. In this case, the *hetwk* and *tdwk* activities, which represent the 9.44% and 10.46% of the entire group dataset respectively, performed remarkably well. For the first activity, only 3% of the instances were incorrectly classified, while the proportion of misclassification for the second activity is 8%. The confusion matrix in Figure 6 indicates



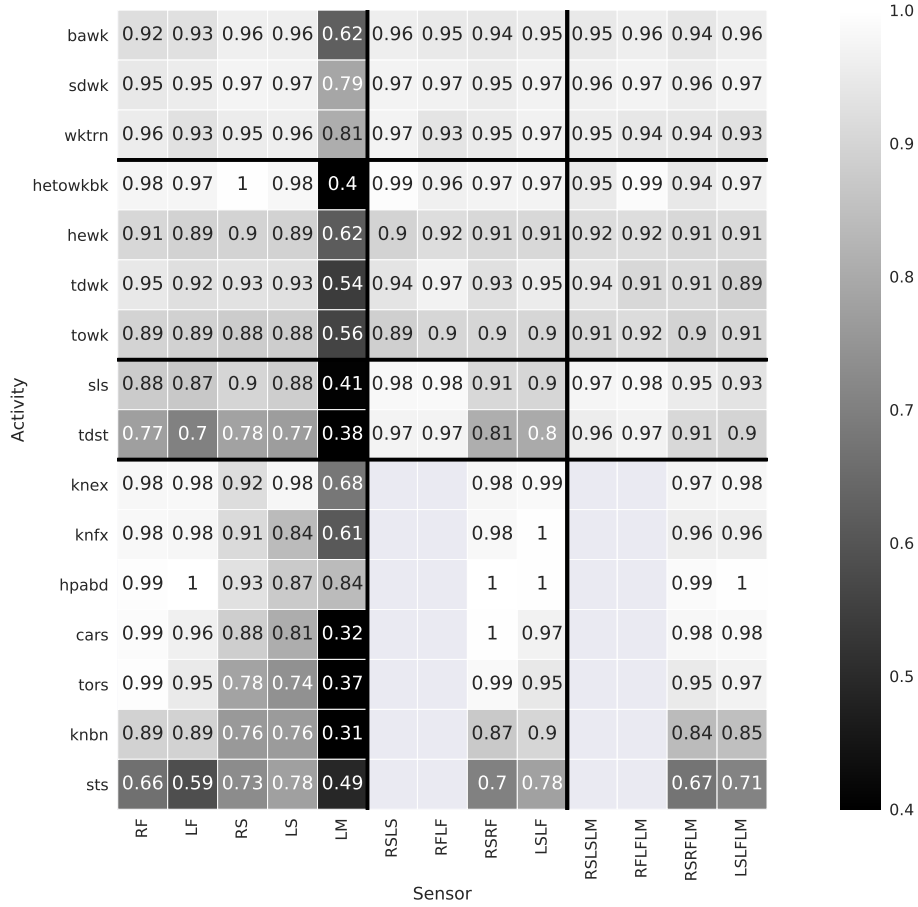


Fig. 4: F-scores for the sensor configurations applied to the activity groups. Empty tiles for the strength group correspond to regions where particular sensor configurations were not applicable (asymmetric activities cannot be classified by using sensors on both the right and the left sides at the same time). The color scheme spans from dark tones of black for low values of F-score, to lighter tones for high F-score values. Lighter tiles denote better results than darker tiles. In order to emphasize small differences in the matrix, the minimum value for the tile color gradient is set to be 0.4 (approximately 0.1 higher than the smallest F-score value), so scores below this value will be marked with a black tile.

True label	bawk	3793	159	39
	sdwk	45	4500	0
	wktrn	47	15	1530
		bawk	sdwk	wktrn
		Predicted label		

Fig. 5: Confusion matrix for the walk group. The left shin sensor was used.

True label	hetowkbk	778	14	6	0
	hewk	0	3592	38	191
	tdwk	0	32	842	32
	towk	0	623	36	3011
		hetowkbk	hewk	tdwk	towk
		Predicted label			

Fig. 6: Confusion matrix for the walking balance group. The combination of right shin and right foot was used.

that the towk and hewk labels, the majority classes, got a rate of false positives of 5% and 17% respectively, in favor of one each other. From the global confusion matrix in Figure 4, these two classes correspond to slightly darker bands within the activity group. As defined in the exercise program, heel walking and toe walking present some similarities.

True label	sls	3921	122
	tdst	308	1899
		sls	tdst
		Predicted label	

Fig. 7: Confusion matrix for the standing balance group. The combination of right shin and right foot was used.

The standing balance group, whose confusion matrix is reported in Figure 7, was not properly classified with a single sensor. The heavy class imbalance, in conjunction with the monotonicity of the signals sampled from these two activities, skewed most of the misclassified instances towards the majority class,

sls, as indicated from the confusion matrix in Figure 7. Nonetheless, the F-scores indicate that symmetric combinations of sensors (right and left foot, right and left shin) were able to discriminate between the two better than the asymmetric ones (right side, left side).

True label	knex	2002	16	0	2	0	3	0
	knfx	43	1661	8	13	0	47	1
	hpabd	0	0	1639	0	0	0	0
	cars	7	6	0	780	0	0	0
	tors	1	0	0	0	708	3	0
	knbn	18	13	0	0	23	2220	507
	sts	0	0	0	0	20	180	861
			knex	knfx	hpabd	cars	tors	knbn
		Predicted label						

Fig. 8: Confusion matrix for the strength group. The combination of left shin, left foot and lumbar sensors was used.

As for the strength group, multiple sensor configurations increased the classification score remarkably when compared with single sensor configurations, in some cases reaching perfect classification for classes such as hpabd, cars or knfx. The two classes that lowered the overall group performance are knbn and sts, as shown in Figure 8. They are based on very similar movements, so weak values of precision and recall are somehow expected.

## 5 Conclusions and Future works

In this paper, we presented a CNN model for the HAR problem. We focused on a set of activities extracted from a common exercise program for fall prevention, training our model data sampled from different sensors, in order to explore the classification capabilities of each individual unit, as well as groups of units. Our experimental results indicate that convolutional models can be used to address the problem of activity recognition in the context of exercise programs. In most cases, combinations of two or three sensors lead to better results compared to the adoption of single inertial units.

Further work on the application of convolutional model to real-world data is recommended. More activities could be included in the workflow, and different aggregations on the activities can be tested. In particular, it is recommended

to diversify the population of participants, in order to validate the classification mechanism to wider age groups. A proper campaign of hyperparameter tuning should be carried over the same set of activities and inertial units, in order to boost the classification performance and reduce the complexity of both the training and inference phases. The very same network structure could be redesigned in an optimized fashion for the task at hand, with particular emphasis on the input adaptation step. As example, shaping the input in a single  $6N \times 204$  could lead to interesting results, as more complex kernels would allow the inclusion of features involving multiple sensors.

## References

1. Abadi, M., Agarwal, A., Barham, P., Brevdo, E., Chen, Z., Citro, C., Corrado, G.S., Davis, A., Dean, J., Devin, M., Ghemawat, S., Goodfellow, I., Harp, A., Irving, G., Isard, M., Jia, Y., Jozefowicz, R., Kaiser, L., Kudlur, M., Levenberg, J., Mané, D., Monga, R., Moore, S., Murray, D., Olah, C., Schuster, M., Shlens, J., Steiner, B., Sutskever, I., Talwar, K., Tucker, P., Vanhoucke, V., Vasudevan, V., Viégas, F., Vinyals, O., Warden, P., Wattenberg, M., Wicke, M., Yu, Y., Zheng, X.: TensorFlow: Large-scale machine learning on heterogeneous systems (2015), <https://www.tensorflow.org/>, software available from tensorflow.org
2. Alsheikh, M.A., Selim, A., Niyato, D., Doyle, L., Lin, S., Tan, H.P.: Deep activity recognition models with triaxial accelerometers. CoRR **abs/1511.04664** (2015), <http://arxiv.org/abs/1511.04664>
3. Banos, O., Galvez, J.M., Damas, M., Pomares, H., Rojas, I.: Evaluating the effects of signal segmentation on activity recognition. In: International Work-Conference on Bioinformatics and Biomedical Engineering, IWBBIO 2014. pp. 759–765 (2014)
4. Bengio, Y.: Practical recommendations for gradient-based training of deep architectures. CoRR **abs/1206.5533** (2012), <http://arxiv.org/abs/1206.5533>
5. Bengio, Y.: Deep learning of representations: Looking forward. CoRR **abs/1305.0445** (2013), <http://arxiv.org/abs/1305.0445>
6. Bulling, A., Blanke, U., Schiele, B.: A tutorial on human activity recognition using body-worn inertial sensors. ACM Comput. Surv. **46**(3), 33:1–33:33 (Jan 2014). <https://doi.org/10.1145/2499621>, <http://doi.acm.org/10.1145/2499621>
7. Burns, A., Greene, B.R., McGrath, M.J., O’Shea, T.J., Kuris, B., Ayer, S.M., Stroiescu, F., Cionca, V.: Shimmer<sup>TM</sup> a wireless sensor platform for non-invasive biomedical research. IEEE Sensors Journal **10**(9), 1527 – 1534 (2010). <https://doi.org/10.1109/JSEN.2010.2045498>
8. Cook, D., Feuz, K.D., Krishnan, N.C.: Transfer learning for activity recognition: a survey. Knowledge and Information Systems **36**(3), 537–556 (Sep 2013). <https://doi.org/10.1007/s10115-013-0665-3>, <https://doi.org/10.1007/s10115-013-0665-3>
9. Godfrey, A., Conway, R., Meagher, D., Laighin, G.: Direct measurement of human movement by accelerometry **30**, 1364–86 (01 2009)
10. Ha, S., Choi, S.: Convolutional neural networks for human activity recognition using multiple accelerometer and gyroscope sensors. In: 2016 International Joint Conference on Neural Networks (IJCNN). pp. 381–388 (July 2016). <https://doi.org/10.1109/IJCNN.2016.7727224>
11. Kingma, D.P., Ba, J.: Adam: A method for stochastic optimization. CoRR **abs/1412.6980** (2014), <http://arxiv.org/abs/1412.6980>

12. Thomas, S., Mackintosh, S., Halbert, J.: Does the otago exercise programme reduce mortality and falls in older adults?: a systematic review and meta-analysis. *Age and Ageing* **39**(6), 681–687 (2010). <https://doi.org/10.1093/ageing/afq102>, <http://dx.doi.org/10.1093/ageing/afq102>
13. Wang, J., Chen, Y., Hao, S., Peng, X., Hu, L.: Deep learning for sensor-based activity recognition: A survey. *CoRR* **abs/1707.03502** (2017), <http://arxiv.org/abs/1707.03502>
14. Yang, J.B., Nguyen, M.N., San, P.P., Li, X.L., Krishnaswamy, S.: Deep convolutional neural networks on multichannel time series for human activity recognition. In: *Proceedings of the 24th International Conference on Artificial Intelligence*. pp. 3995–4001. *IJCAI'15*, AAAI Press (2015), <http://dl.acm.org/citation.cfm?id=2832747.2832806>
15. Zeng, M., Nguyen, L.T., Yu, B., Mengshoel, O.J., Zhu, J., Wu, P., Zhang, J.: Convolutional neural networks for human activity recognition using mobile sensors. In: *6th International Conference on Mobile Computing, Applications and Services*. pp. 197–205 (Nov 2014). <https://doi.org/10.4108/icst.mobicase.2014.257786>